Thermoresponsive Micellization of Poly(ethylene glycol)-*b*-poly(*N*-isopropylacrylamide) in Water

Wangqing Zhang, Linqi Shi,* Kai Wu, and Yingli An

Key Laboratory of Functional Polymer Materials, Institute of Polymer Chemistry, N&T Joint Academy, Nankai University, Tianjin 300071, China

Received May 2, 2005

ABSTRACT: Thermoresponsive micellization of poly(ethylene glycol)-*b*-poly(*N*-isopropylacrylamide) (PEG_{110}-*b*-$PNIPAM_{44}$) in water is studied by static light scattering and dynamic light scattering. The critical aggregation temperature of PEG_{110}-*b*-$PNIPAM_{44}$ is a little higher than homopolymer PNIPAM, and it depends on the block copolymer concentration, which increases from 33.7 to 38.4°C when the copolymer concentration decreases from 2.0 to 0.20 mg/mL. Above the critical aggregation temperature, thermoresponsive micellization occurs, and the resultant spherical micelles consist of a PNIPAM core and a PEG shell. The block copolymer concentration exerts a strong influence on the size and structure of the resultant micelles. Micellization of PEG_{110}-*b*-$PNIPAM_{44}$ at higher copolymer concentration favors formation of narrowly distributed, small, and dense micelles, while large, loose micelles or micellar clusters form at lower block copolymer concentration.

1. Introduction

Micellization of hydrophobic−hydrophilic block copolymers or amphiphilic block copolymers in block-selective solvents and the resultant micelles are well documented in scientific literature in the past 20 years.[1] Usually, micellization of amphiphilic block copolymers in block-selective solvent produces core−shell micelles, where the insoluble block forms the core and the soluble block forms the shell of the resultant core−shell micelles.[1] Besides amphiphilic block copolymers, micellization of hydrophilic−hydrophilic block copolymers, which are also called double hydrophilic block copolymers, are also widely studied recently.[2] Usually, hydrophilic−hydrophilic block copolymers behave as single chains in aqueous solution like classical polymers or polyelectrolytes, whereas its micellization similar to that of amphiphilic block copolymers can occur under the influence of a given external stimuli, mainly temperature, pH, ionic strength changes, or complexation.[2,3]

Of all the hydrophilic−hydrophilic block and graft copolymers, poly(ethylene glycol)-*b*-poly(*N*-isopropylacrylamide) (PEG-*b*-PNIPAM) or poly(ethylene glycol)-*g*-poly(*N*-isopropylacrylamide) (PEG-*g*- PNIPAM) is an interesting one, where the PNIPAM is one of the most studied responsive polymers that exhibits a lower critical solution temperature (LCST) in water around 32°C and the PEG is usually used for the stabilization of dispersions and emulsions.[4,5] Below the LCST of the PNIPAM block, PEG-*b*-PNIPAM or PEG-*g*-PNIPAM is highly soluble in aqueous solution, while above the LCST, the thermosensitive PNIPAM block precipitates, and the copolymer self-assembles into polymeric micelles, which consist of a PNIPAM core and a hydrophilic shell of PEG.[6] The thermoresponsive aggregation of PEG-*b*-PNIPAM or PEG-*g*-PNIPAM has been studied extensively. For example, Tenhu et al. studied the aggregation of PEG-*b*-PNIPAM in water by fluorescence spectroscopy and light scattering;[6a] Zhu and Napper studied the gelation of PEG-*b*-PNIPAM;[7] Wu et al. studied the formation of core−shell nanoparticles of PEG-*g*-PNIPAM through the coil to globule transition of the PNIPAM block;[6c] Feijen et al. studied the thermosensitive micelle formation of PEG-*b*-PNIPAM.[6d] However, the copolymers used in the study mentioned above usually have relatively high molecular weight of PNIPAM block of the copolymers. For example, the molecular weight of the PNIPAM block was as high as $1 \times 10^{5-6}$ g/mol.[5−7] Herein, we study the thermoresponsive micellization of PEG-*b*-PNIPAM with low and narrowly distributed molecular weight of PNIPAM block by laser lighting scattering. It is found the critical aggregation temperature of PEG_{110}-*b*-$PNIPAM_{44}$ depends on block copolymer concentration. Besides, the size of the resultant PEG-*b*-PNIPAM micelles decreases when the block copolymer concentration increases, which is different than the gelation of PEG-*b*-PNIPAM or PEG-*b*-PNIPAM with high molecular weight of PNIPAM block.

2. Experimental Section

Materials. Polyethylene glycol monomethyl ether (CH_3O−PEG_{110}−OH) (M_w = 5000 and the polydispersity index PDI = 1.05) was purchased from Fluka. CuCl was purchased from Aldrich and purified according to ref 8. Tris[2-(dimethylamino)-ethyl]amine (Me_6TREN) was synthesized according to ref 8. The monomer *N*-isopropylacrylamide (NIPAM, Acros Organics) was purified by recrystallization in a benzene/*n*-hexane mixture and dried carefully in a vacuum. All water used in this study was purified with a Millipore Mill-Q system, and the resistivity was above 16 MΩ cm. Other reagents were used as received.

Synthesis of PEG Macroinitiator. The macroinitiator PEG_{110}-Br was synthesized according to ref 9. The synthetic procedures and the H NMR spectrum of PEG_{110}-Br can be found in the Supporting Information.

Synthesis of PEG_{110}-*b*-$PNIPAM_{44}$. PEG_{110}-*b*-$PNIPAM_{44}$ was synthesized by atom transfer radical polymerization (ATRP). The typical polymerization procedure was introduced as follows. 5.0 g of PEG_{110}-Br was added into a reaction flask, and then a 10 mL solvent mixture of butanone and 2-propanol (1:1 by volume) was added. The sample was first stirred and then degassed under nitrogen purge. Subsequently, the CuCl and Me_6TREN catalysts (0.148 g of CuCl and 0.345 g of Me_6-

* To whom correspondence should be addressed. E-mail: shilinqi@nankai.edu.cn.

10.1021/ma0509199 CCC: $30.25
Published on Web 06/02/2005

TREN) were introduced into the reaction flask. At last, 6.5 g of NIPAM was added into the flask and degassed under nitrogen purge. Polymerization was performed at 40 °C for 48 h, and NIPAM conversion was about 70%. The block copolymer PEG_{110}-*b*-$PNIPAM_{44}$ was purified by first passing through an Al_2O_3 column to remove the copper catalyst and then precipitated in cold ether. The PDI of PEG_{110}-Br and PEG_{110}-*b*-$PNIPAM_{44}$ measured by gel permeation chromatography (GPC) (see the GPC chromatograms in the Supporting Information) was 1.05 and 1.06, respectively, where tetrahydrofuran was used as eluent and narrow-polydispersity polystyrene was used for calibration standard. The composition of the block copolymer PEG_{110}-*b*-$PNIPAM_{44}$ was determined by the ^1H NMR spectrum, as shown in the Supporting Information.

Light Scattering Measurement. The block copolymer PEG_{110}-*b*-$PNIPAM_{44}$ was dissolved in water at room temperature (about 18 °C) to make up a series of aqueous solutions with block copolymer concentration ranging from 0.20 to 2.0 mg/mL. All samples were first prepared by filtering about 1 mL of the aqueous solution with a 0.45 μm Millipore filter into a clean scintillation vial and heating at different temperatures for a given time and then characterized by a combination of static laser scattering (SLS) and dynamic laser scattering (DLS).

In DLS measurement, the Laplace inversion of a measured intensity−intensity time correlation function $G^{(2)}(t,q)$ in the self-beating mode can result in a line-width distribution $G(\Gamma)$. For a pure diffusive relation, $G(\Gamma)$ can be transferred into a translational diffusion coefficient distribution $G(D)$ since $\Gamma/q^2_{\theta\to0,C\to0} \to D$ or a hydrodynamic diameter distribution $f(D_h)$ via the Stokes−Einstein equation

$$D_h = k_b T/(3\pi\eta D) \tag{1}$$

where k_b, T, and η are the Boltzmann constant, the absolute temperature, and the solvent viscosity, respectively. In the present study, $\Gamma/q^2_{\theta\to0}$ or D^0 of the micelles at given concentration was calculated by extrapolating q^2 to 0, and then the hydrodynamic diameter D_h^0 or the hydrodynamic diameter distribution $f(D_h)$ of the micelles at given polymer concentration was further calculated from eq 1. The radius of gyration R_g, the second virial coefficient A_2, and the weight-average molar mass of the micelles M_w were calculated from SLS. On the basis of SLS theory, for a relatively dilute macromolecule solution at polymer concentration C (g/mL) and at the scattering angle θ, the angular dependence of the excess absolute average scattered intensity, known as the excess Rayleigh ratio $R(\theta,C)$, can be approximated as

$$[KC/R(\theta,C)] = [1/M_w][1 + (R_g^2q^2)/3] + 2A_2C \tag{2}$$

where K is the optical constant and $K = 4\pi^2n^2(dn/dc)^2/(N_A\lambda_0^4)$ with N_A, n, and λ_0 being Avogadro's number, the solvent refractive index, and the wavelength of laser, respectively; dn/dc is the specific refractive index increment, and q is the magnitude of the scattering wave vector, $q = (4\pi n/\lambda_0)\sin(\theta/2)$. For a given dilute polymer solution, eq 2 can be expressed as

$$[KC/R(\theta,C)] \approx [1/M_w][1 + (R_g^2q^2)/3] \tag{3}$$

On the basis of eq 3, the apparent radius of gyration R_g and apparent weight-average molar mass M_w of the micelles were calculated after measuring $R(\theta,C)$ at a set of θ series.

In this study, DLS and SLS measurements were performed on a laser light scattering spectrometer (BI-200SM) equipped with a digital correlator (BI-9000AT) at 514 nm. The detailed method of DLS and SLS measurements can be seen in our recent works or Wu's study.[10]

3. Results and Discussion

3.1. The Critical Aggregation Temperature of PEG_{110}-*b*-$PNIPAM_{44}$. Figure 1 shows the hydrodynamic diameter distribution $f(D_h)$ of PEG_{110}-*b*-$PNIPAM_{44}$ in water at 25 °C. The hydrodynamic diameter D_h of PEG_{110}-*b*-$PNIPAM_{44}$ ranges from 7.5 to 7.9 nm, and the apparent hydrodynamic diameter D_h^{app} can be calculated from $f(D_h)$ by $\int_0^\infty f(D_h)D_h\, dD_h$, which is about 7.7 nm. Since the LCST of PNIPAM in water is about 32 °C and the PEG and PNIPAM blocks are soluble in water at 25 °C,[4] the average hydrodynamic diameter of the coils of single chains of PEG_{110}-*b*-$PNIPAM_{44}$ is about 7.7 nm.

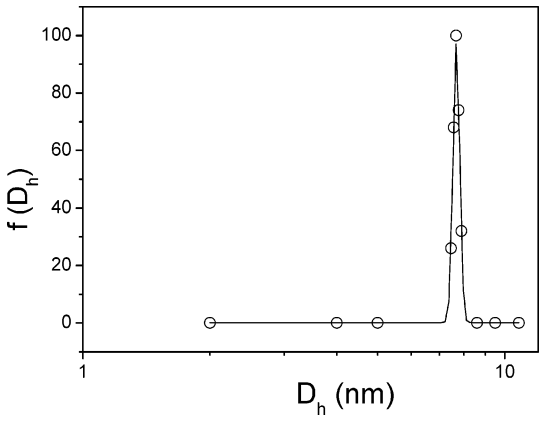

Figure 1. Hydrodynamic diameter distribution $f(D_h)$ of the coils of single chains of PEG_{110}-*b*-$PNIPAM_{44}$ in water at 25 °C.

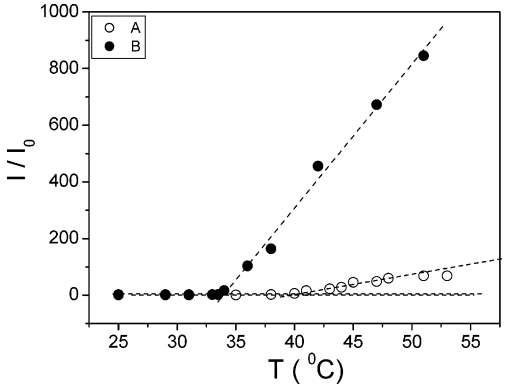

Figure 2. Temperature dependence of the normalized intensity I/I_0 of PEG_{110}-*b*-$PNIPAM_{44}$ at 0.20 mg/mL (○) and 2.0 mg/mL (●), respectively.

Figure 2 shows the temperature dependence of the normalized intensity of PEG_{110}-*b*-$PNIPAM_{44}$ at two block copolymer concentrations of 0.20 mg/mL (A) and 2.0 mg/mL (B), where the block copolymer aqueous solution was heated for about 60 min at each temperature, and then the scattering intensity was measured. Clearly, the sharp increase of the scattering intensity implies the occurrence of micellization, and the critical aggregation temperatures of PEG_{110}-*b*-$PNIPAM_{44}$ with polymer concentration at 0.20 and 2.0 mg/mL are 38.4 and 33.7 °C, respectively. Compared with the homopolymer of PNIPAM, the critical aggregation temperature of PEG_{110}-*b*-$PNIPAM_{44}$ is a little higher, which is possibly due to the soluble PEG block in water. Furthermore, it is also found that the critical aggregation temperature ranges from 38.4 to 33.7 °C when the copolymer concentration increases from 0.20 to 2.0 mg/mL. The results suggest that the critical aggregation temperature of PEG_{110}-*b*-$PNIPAM_{44}$ is higher at lower block copolymer concentrations, which is consistent with the results achieved by Zhu and Napper.[7] The results

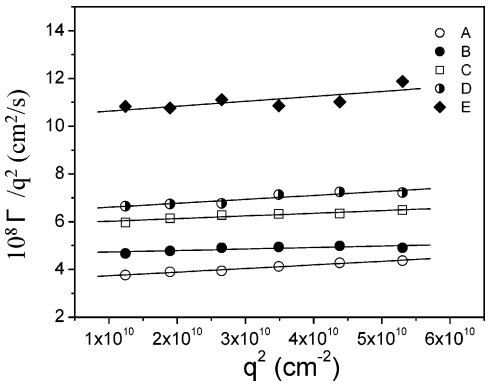

Figure 3. Plots of Γ/q^2 vs q^2 of the PEG_{110}-*b*-$PNIPAM_{44}$ micelles formed at block copolymer concentration of 0.20 (A), 0.40 (B), 0.80 (C), 1.20 (D), and 2.0 mg/mL (E) at 47 °C.

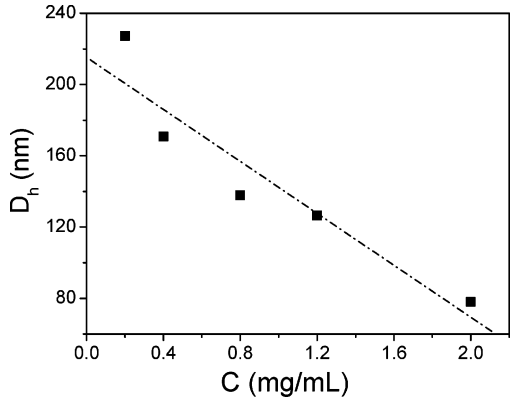

Figure 4. Block copolymer concentration dependence of the hydrodynamic diameter D_h of the PEG_{110}-*b*-$PNIPAM_{44}$ micelles formed at 47 °C.

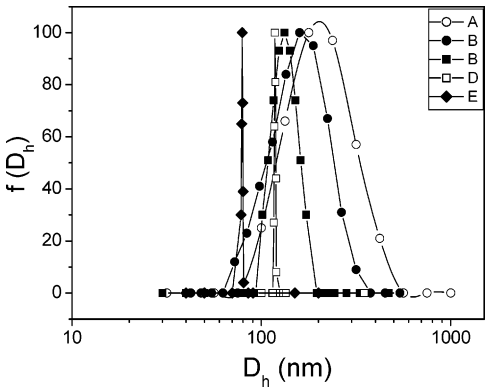

Figure 5. Hydrodynamic diameter distribution $f(D_h)$ of the PEG_{110}-*b*-$PNIPAM_{44}$ micelles formed at block copolymer concentration of 0.20 (A), 0.40 (B), 0.80 (C), 1.20 (D), and 2.0 mg/mL (E) at 47 °C.

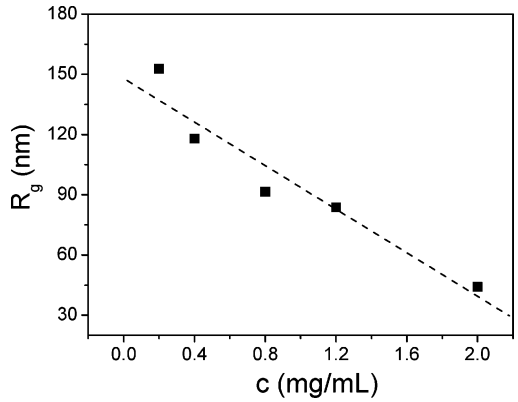

Figure 6. Block copolymer concentration dependence of the radius of gyration R_g of the PEG_{110}-*b*-$PNIPAM_{44}$ micelles formed at 47 °C.

also mean that micellization of PEG_{110}-*b*-$PNIPAM_{44}$ occurs easily at higher copolymer concentration.

3.2. The PEG_{110}-*b*-$PNIPAM_{44}$ Micelles. Hennink et al. have found that micellization of PEG-*b*-PNIPAM at high temperature favors formation of narrowly distributed micelles.[11] Thus, in the following study, the sample of about 1 mL of aqueous solution of PEG_{110}-*b*-$PNIPAM_{44}$ was bathed at 47 °C, which is much higher than the critical aggregation temperature of PEG_{110}-*b*-$PNIPAM_{44}$, and then the resultant micelles are studied. Figure 3 shows the plots of Γ/q^2 vs q^2 of the PEG_{110}-*b*-$PNIPAM_{44}$ micelles formed at different block copolymer concentrations at 47 °C. From the fit lines in Figure 3, the values of the translational diffusion coefficient D^0 of the resultant micelles formed at block copolymer concentration of 0.20, 0.40, 0.80, 1.20, and 2.0 mg/mL can be calculated by extrapolating q^2 to 0, which are 3.58×10^{-8}, 4.67×10^{-8}, 5.91×10^{-8}, 6.44×10^{-8}, and 10.42×10^{-8} cm^2/s, respectively. It is also found that the Γ/q^2 values of the PEG_{110}-*b*-$PNIPAM_{44}$ micelles formed at different block copolymer concentrations are almost independent of q^2, which suggests that the micelles are spherical.[12] Besides, based on eq 1, the values of the hydrodynamic diameter D_h of the PEG_{110}-*b*-$PNIPAM_{44}$ micelles formed at different copolymer concentrations can be calculated, and the values are shown in Figure 4.

It can be clearly seen in Figure 4 that the hydrodynamic diameter D_h of the resultant PEG_{110}-*b*-$PNIPAM_{44}$ micelles decreases from 227 to 78 nm when the block copolymer concentration increases from 0.20 to 2.0 mg/mL. Thus, the micellization of PEG_{110}-*b*-$PNIPAM_{44}$ is very different than the aggregation of the PEG-*b*-PNIPAM or PEG-*g*-PNIPAM with a high molecular weight PNIPAM block, where the diameter of the resultant micelles or nanoparticles usually increases at higher block copolymer concentration.[6,7] We think the reason that large-sized micelles formed at lower copolymer concentration is possibly due to the relatively slow micellization of PEG_{110}-*b*-$PNIPAM_{44}$.

Figure 5 shows the hydrodynamic diameter distribution $f(D_h)$ of the PEG_{110}-*b*-$PNIPAM_{44}$ micelles formed at block copolymer concentration ranging from 0.20 to 2.0 mg/mL at 47 °C. Clearly, the hydrodynamic diameter of the PEG_{110}-*b*-$PNIPAM_{44}$ micelles decreases with increasing block copolymer concentration. Besides, the hydrodynamic diameter distribution $f(D_h)$ of the PEG_{110}-*b*-$PNIPAM_{44}$ micelles becomes progressively narrower with increasing block copolymer concentration. In fact, the PEG_{110}-*b*-$PNIPAM_{44}$ micelles formed at block copolymer concentration of 2.0 mg/mL is narrowly distributed with a relative width μ_2/Γ^2 lower than 0.05. This means that micellization of PEG_{110}-*b*-$PNIPAM_{44}$ at high polymer concentration favors formation of small, narrowly distributed core−shell micelles.

Figure 6 shows the apparentradius of gyration R_g of the PEG_{110}-*b*-$PNIPAM_{44}$ micelles formed at different block copolymer concentrations at 47 °C. Clearly, the R_g of the resultant micelles decreases from 153 to 44 nm as the block copolymer concentration increases from 0.20 to 2.0 mg/mL. It is well-known that the R_g/R_h value, where R_h is the hydrodynamic radius, indicates the particle shape in solution.[13−16] The R_g/R_h value of the PEG_{110}-*b*-$PNIPAM_{44}$ micelles as shown in Figure 7

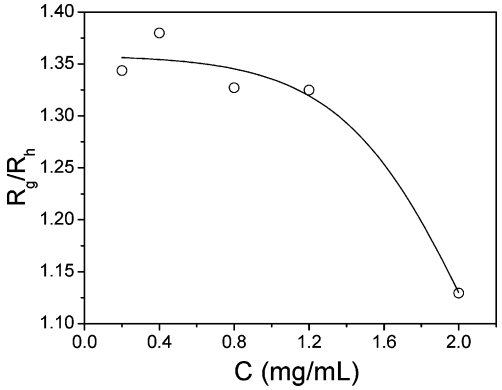

Figure 7. R_g/R_h value of the PEG_{110}-*b*-$PNIPAM_{44}$ micelles formed at different block copolymer concentrations.

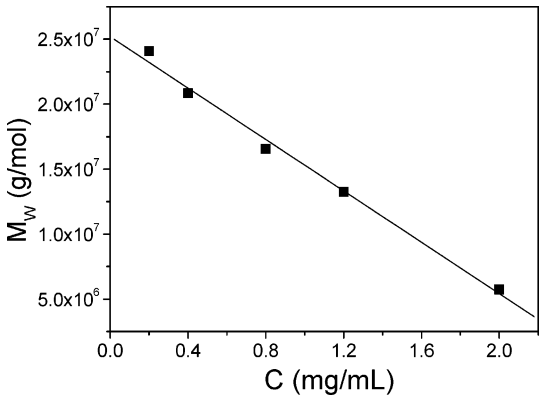

Figure 8. Block copolymer concentration dependence of the apparent weight-average molar mass M_w of the PEG_{110}-*b*-$PNIPAM_{44}$ micelles formed at 47 °C.

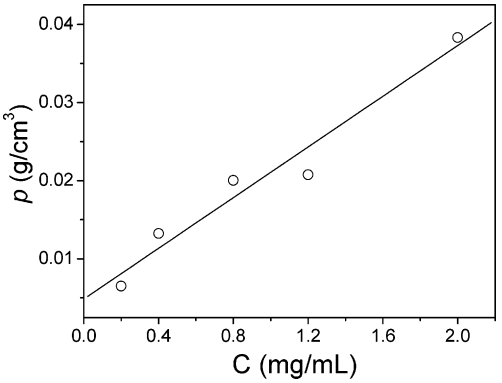

Figure 9. Block copolymer concentration dependence of the chain density ρ of the PEG_{110}-*b*-$PNIPAM_{44}$ micelles formed at 47 °C.

decreases from 1.38 to 1.13 when the block copolymer concentration increases from 0.20 to 2.0 mg/mL. In comparison with random coils of homopolymers ($R_g/R_h \sim 1.50$),[13] the R_g/R_h value of the PEG_{110}-*b*-$PNIPAM_{44}$ micelles is much smaller, which confirms the formation of the micelles. However, compared with typical amphiphilic block copolymer crew-cut micelles (~ 0.775)[12,13] or the aggregates of homopolymer PNIPAM (~ 0.62) formed above its LCST,[17] the R_g/R_h value of the PEG_{110}-*b*-$PNIPAM_{44}$ micelles is much bigger, which is possibly due to the relatively long coronal PEG block. We think the larger aggregates formed at low concentration of PEG_{110}-*b*-$PNIPAM_{44}$ are possibly loose compound micelles or micellar clusters,[15,16] while the smaller aggregates formed at high polymer concentration of 2.0 mg/mL are well-defined micelles.

Assuming that the specific refractive index increment (dn/dc) of the micelles can be approximately expressed as[6a]

$$dn/dc = w_A(dn/dc)_A + w_B(dn/dc)_B \quad (4)$$

in which w_A and w_B are the mass fractions of the PNIPA and PEG block and $(dn/dc)_A$ and $(dn/dc)_B$ are their refractive index increments, respectively; the dn/dc value of PEG_{110}-*b*-$PNIPAM_{44}$ in water can be calculated. Besides, the temperature dependence on dn/dc of the block copolymer has also been observed to be minimal;[6c] this justifies the use of eq 4. In the present study, the dn/dc value is calculated to be 0.161. Thus, the apparent weight-average molar mass M_w of the PEG_{110}-*b*-$PNIPAM_{44}$ micelles can be calculated by a Zimm plot, which is shown in Figure 8. The results suggest that the apparent M_w of the PEG_{110}-*b*-$PNIPAM_{44}$ micelles linearly decreases from 2.41×10^7 to 5.76×10^6 g/mol as the block copolymer concentration increases from 0.20 to 2.0 mg/mL.

The polymer chain density ρ of the PEG_{110}-*b*-$PNIPAM_{44}$ micelles, which is calculated as $\rho = M_w/(N_A\pi/6D_h^3)$,[6c] is shown in Figure 9. The results show the chain density ρ of the PEG_{110}-*b*-$PNIPAM_{44}$ micelles linearly increases from 6.53×10^{-3} to 3.83×10^{-2} g/cm^3 when the block copolymer concentration increases from 0.20 to 2.0 mg/mL. On the basis of all the results such as the hydrodynamic diameter D_h, radius of gyration R_g, the R_g/R_h value, the apparent M_w, and the chain density ρ of the PEG_{110}-*b*-$PNIPAM_{44}$ micelles formed at different copolymer concentrations, it can be concluded that micellization of PEG_{110}-*b*-$PNIPAM_{44}$ at high block copolymer concentration favors formation of small narrowly distributed, compact micelles, while large, loose micelles or micellar clusters form at low block copolymer concentration.

4. Conclusions

The thermoresponsive micellization of PEG_{110}-*b*-$PNIPAM_{44}$ in water above the critical aggregation temperature of the PNIPAM block forms spherical core–shell micelles with the PNIPAM block as core and the PEG block as shell. The critical aggregation temperature of PEG_{110}-*b*-$PNIPAM_{44}$ is a little higher than that of the PNIPAM homopolymer, and the temperature depends on the block copolymer concentration. The critical aggregation temperature increases from 33.7 to 38.4°C when the copolymer concentration decreases from 2.0 to 0.20 mg/mL. The block copolymer concentration exerts a strong influence on the size and structure of the PEG_{110}-*b*-$PNIPAM_{44}$ micelles. The micellization of PEG_{110}-*b*-$PNIPAM_{44}$ at high copolymer concentration favors formation of narrowly distributed, small, dense micelles, while large, loose micelles or micellar clusters form at low block copolymer concentration.

Acknowledgment. The financial support by the Outstanding Scholar Program of Nankai University, National Natural Science Foundation of China (No. 50273015, 20474032, and 23028407), and Chinese Education Ministry Foundation for Nankai University and Tianjin University Joint Academy is gratefully acknowledged.

Supporting Information Available: Text giving synthetic procedures for the macroinitiator PEG_{110}-Br; figures showing ^1H NMR spectra of PEG_{110}-Br and PEG_{110}-*b*-$PNIPAM_{44}$ and the GPC chromatogram of PEG_{110}-Br and PEG_{110}-*b*-$PNIPAM_{44}$. This material is available free of charge via the Internet at http://pubs.acs.org.

References and Notes

(1) (a) *Solvents and Self-Organization of Polymers*; Webber, S. E., Munk, P., Tuzar, Z., Eds.; NATO ASI Series E; Kluwer Academic Publishers: Dordrecht, 1996; Vol. 327. (b) Zhang, L.; Eisenberg, A. *Science* **1995**, *268*, 1728. (c) Zhou, Z.; Li, Z.; Ren, Y.; Hillmyer, M. A.; Lodge, T. P. *J. Am. Chem. Soc.* **2003**, *125*, 10182. (d) Borisov, O. V.; Zhulina, E. B. *Macromolecules* **2003**, *36*, 10029. (e) Tao, J.; Stewart, S.; Liu, G.; Yang, M. *Macromolecules* **1997**, *30*, 2738. (f) Zhang, W.; Shi, L.; An, Y.; Gao, L.; Wu, K.; Ma, R. *Macromolecules* **2004**, *37*, 2551.

(2) (a) Forder, C.; Patrickios, C. S.; Billingham, N. C.; Armes, S. P. *Chem. Commun.* **1996**, *7*, 883. (b) Gohy, J.-F.; Varshney, S. K.; Jerome, R. *Macromolecules* **2001**, *34*, 3361. (c) Ranger, M.; Jones, M. C.; Yessine, M. A.; Leroux, J. C. *J. Polym. Sci., Part A* **2001**, *39*, 3861. (d) Martin, T. J.; Prochazka, K.; Munk, P.; Webber, S. E. *Macromolecules* **1996**, *29*, 6071. (e) Vamvakaki, M.; Billingham, N. W.; Armes, S. P. *Macromolecules* **1999**, *32*, 2088. (f) Liu, S.; Billingham, N. C.; Armes, S. P. *Angew. Chem., Int. Ed.* **2001**, *40*, 2328.

(3) (a) Zhang, Y.; Xiang, M.; Jiang, M.; Wu, C. *Macromolecules* **1997**, *30*, 6084. (b) Harada, A.; Kataoka, K. *Macromolecules* **2003**, *36*, 4995. (c) Stapert, H. R.; Nishiyama, N.; Jiang, D.; Aida, T.; Kataoka, K. *Langmuir* **2000**, *16*, 8182. (d) Zhang, W.; Shi, L.; Gao, L.; An, Y.; Li, G.; Wu, K.; Liu, Z. *Macromolecules* **2005**, *38*, 6084.

(4) (a) Kubota, K.; Fujishige, S.; Ando, I. *J. Phys. Chem.* **1990**, *94*, 5154. (b) Wu, C.; Zhou, S. *Macromolecules* **1995**, *28*, 5388. (c) Schild, H. G. *Prog. Polym. Sci.* **1992**, *17*, 163. (d) Wu, C.; Qiu, X. P. *Phys. Rev. Lett.* **1998**, *80*, 620.

(5) (a) Jankova, K.; Chen, X.; Kops, J.; Batsberg, W. *Macromolecules* **1998**, *31*, 538. (b) Uhrich, K. E.; Cannizzaro, S. M.; Langer, R. S.; Shakesheff, K. M. *Chem. Rev.* **1999**, *99*, 3181. (c) Bromberg, L. E.; Ron, E. S. *Adv. Drug Delivery Rev.* **1998**, *31*, 197.

(6) (a) Virtanen, J.; Holappa, S.; Lemmetyinen, H.; Tenhu, H. *Macromolecules* **2002**, *35*, 4763. (b) Liang, D.; Zhou, S.; Song, L.; Zaitsev, V. S.; Chu, B. *Macromolecules* **1999**, *32*, 6326. (c) Qiu, X.; Wu, C. *Macromolecules* **1997**, *30*, 7921. (d) Topp, M. D. C.; Dijkstra, P. J.; Talsma, H.; Feijen, J. *Macromolecules* **1997**, *30*, 8518.

(7) (a) Zhu, P. W.; Napper, D. H. *Macromolecules* **1999**, *32*, 2068. (b) Zhu, P. W.; Napper, D. H. *Langmuir* **2000**, *16*, 8543.

(8) Xia, J.; Zhang, X.; Matyjaszewski, K. *Macromolecules* **1999**, *32*, 3531.

(9) Liu, S.; Weaver, J. V. M.; Save, M.; Armes, S. P. *Langmuir* **2002**, *18*, 8350.

(10) (a) Zhang, W.; Shi, L.; An, Y.; Gao, L.; Wu, K.; Ma, R.; He, B. *Phys. Chem. Chem. Phys.* **2004**, *6*, 109. (b) Zhang, W.; Shi, L.; An, Y.; Wu, K.; Gao, L.; Liu, Z.; Ma, R.; Meng, Q.; Zhao, C.; He, B., *Macromolecules* **2004**, *37*, 2924. (c) Zhang, G.; Wu, C. *J. Am. Chem. Soc.* **2000**, *122*, 10201.

(11) Neradovic, D.; Soga, O.; Nostrum, C. F. Van, Hennink, W. E. *Biomaterials* **2004**, *25*, 2409.

(12) Xu, R.; Winnik, M. A.; Hallett, F. R.; Riess, G.; Croucher, M. D. *Macromolecules* **1991**, *24*, 87.

(13) Tu, Y.; Wan, X.; Zhang, D.; Zhou, Q.; Wu, C. *J. Am. Chem. Soc.* **2000**, *122*, 10201.

(14) Wu, C.; Zuo, J.; Chu, B. *Macromolecules* **1989**, *22*, 633.

(15) Antonietti, M.; Heinz, S.; Schimidt, M. *Macromolecules* **1990**, *23*, 3796.

(16) Antonietti, M.; Wremser, W.; Schimidt, M.; Rosenauer, C. *Macromolecules* **1994**, *27*, 3276.

(17) Wu, C.; Zhou, S. *Macromolecules* **1995**, *28*, 8381.

MA0509199